ACADEMIA ROMÂNĂ
Revue Roumaine de Chimie
http://web.icf.ro/rrch/

Rev. Roum. Chim.,
2012, 57(12), 1057-1064

ELECTROCHEMICAL AND SEM CHARACTERIZATION OF PLASMA SPRAYED YsZ COATING

Geanina Laura PINTILEI,[a] Daniel MARECI,[b,*]
Sorin Claudiu IACOB STRUGARU[a] and Corneliu MUNTEANU[a]

[a] "Gheorghe Asachi" Technical University of Iaşi, Faculty of Mechanical Engineering,
61-63 Prof. dr. doc. D. Mangeron Blvd, 700050, Iaşi, Roumania
[b] "Gheorghe Asachi" Technical University of Iaşi, Faculty of Chemical Engineering and Environmental Protection,
73 Prof. dr. doc. D. Mangeron Blvd, 700050, Iaşi, Roumania

Received October 1, 2012

Linear polarization and electrochemical impedance spectroscopy (EIS) were employed to characterize the electrochemical behavior of plasma sprayed yttrium oxide stabilized zirconium oxide (YsZ) coated 310 austenitic stainless steel in 3.5% NaCl solution. Surface characterization before and after electrochemical testing was performed used scanning electron microscopy (SEM). 310 austenitic stainless steel substrate showed higher zero corrosion potential (ZCP) and lower corrosion current density (icorr) compared with the YsZ-coated. The reason for that is the penetrations of corrosive solution into the 310 austenitic stainless steel surface alloy through the pores. The electrochemical properties of the coated 310 austenitic stainless steel sample at the open circuit potential at different immersion time in 3.5% NaCl solution were studied by EIS. Equivalent circuit (EC) was used to modeling EIS data, in order to characterize YsZ-coated 310 austenitic stainless steel surface.

INTRODUCTION

Ceramic coatings have been extensively used as metallic structural components for construction, automotive and aerospace application. Such coatings are used to protect internal components from corrosion and friction under severe condition such as temperature and corrosive medium. ZrO_2 (zirconia) is a ceramic and have properties such as superior refractoriness, good mechanical strength, high ionic conductivity, low thermal conductivity, high thermal expansion coefficient and excellent corrosion resistance.[1, 2]

Commercial ZrO_2 ceramics are basically classified as partial stabilized zirconia and tetragonal zirconia polycrystals. The addition of "stabilizing" oxide, like CaO, MgO and Y_2O_3 to pure ZrO_2 allows generating multiphase materials, but in last years the research efforts appeared to be more focused on Zr_2O_3-Y_2O_3 ceramics.[3]

Sputtering,[4] plasma spraying,[5] laser ablation[6] metal organic chemical vapor deposition,[7] and sol-gel[8,9] methods, good ZrO_2 thin films and coatings can be prepared for different applications.

Ceramic coatings generated by plasma spraying have been used as anti-corrosion layers for metallic components.[10,11] The disadvantages associated with plasma spraying of ceramic coatings are the rapid solidification of the flight particles.

An aerated 3.5% NaCl solution was chosen as corrosive medium, bearing in mind that the chloride ion is present in many corrosion situations. There are two competitive processes that operate simultaneously in chloride environments: the chloride ion activity – which tends to destroy the passive film and the dissolved oxygen – which acts to promote and repair the passive film on metallic materials of construction. The electrochemical methods have been shown in numerous studies to be an efficient and convincing

* Corresponding author: danmareci@yahoo.com

tool for analyzing the corrosion behavior of metals or alloys.[12-15]

This paper concentrates on the evaluation of the electrochemical behavior of yttrium oxide stabilized zirconium oxide (YsZ) coating by plasma sprayed on 310 austenitic stainless steel. The corrosion characteristics of this material were first investigated by standard potentiodynamic polarization technique, and next by electrochemical impedance spectroscopy (EIS) in 3.5% NaCl solution at 25 ^{o}C.

MATERIALS AND METHODS

Materials

310 austenitic stainless steel was used in these tests as the substrate material. 310 austenitic stainless steel were mirror-polished (with 400 to 2000 grit emery paper and alumina suspension), washed with bi-distilled water, ultrasonically degreased in ethanol and dried in air. The layers on 310 austenitic stainless steel by plasma spray system (SPRAYWIZARD-9MCE, Sultzer-Metco, USA) were obtained from bulks samples of YsZ produced by Sultzer-Metco, USA. The YsZ coated was deposited at the Faculty of Mechanical Engineering of Iaşi.

The spray parameters are listed in Table 1. The YsZ was sprayed continuously by moving the plasma gun, attached to a programmable robot, in front of the NiMo substrate.

The uncoated 310 austenitic stainless steel, again, were mirror-polished (with 400 to 2000 grit emery paper and alumina suspension), washed with bi-distilled water, ultrasonically degreased in ethanol and dried in air. Both, coated and uncoated tests specimens were embedded in a polytetrafluoroethylene (PTFE) holder specifically designed to connect to a rotating disc electrode (type EDI 101T; Radiometer Analytical, France). A polymeric resin was used to ensure a tight seal between the specimen and the PTFE holder, to avoid crevice corrosion.[16]

Coating characterization

XRD spectra were recorded using an X'Pert PRO MRD, PANalytical Holland diffractometer and Cu K_{α} radiation. The surfaces of YsZ-coated before and after electrochemical characterization were investigated using a Quanta 3D scanning electron microscope (model AL99/D8229).

Electrochemical characterization

Corrosion tests were performed electrochemically at room temperature (~ 25 ^{o}C) in a 3.5% NaCl in distilled water.

The test specimens were placed in a glass corrosion cell, which was filled with freshly prepared electrolyte. A saturated calomel electrode (SCE) was used as the reference electrode and a platinum coil as the counter electrode. All potentials referred to in this article are with respect to SCE. The measurement was managed by a VoltaLab 40 potentiostat controlled by a personal computer with dedicate software (VoltaMaster 4).

For both samples (coated and uncoated) linear potentiodynamic polarization measurement was performed. These tests were conducted by stepping the potential using a scanning rate of 1 mV/s from -1000 mV (SCE) to +1000 mV (SCE).

EIS measurements were performed after the samples were immersed in both electrolytes at 25±1^{o}C, at open circuit potential, for different period of times. The alternating current (AC) impedance spectra for samples were obtained with a scan frequency range of 100 kHz to 10 mHz with amplitude of 10 mV.

Table 1

Spray parameters used for plasma spray YsZ coatings

Internal	Feeding mode
Arc current (A)	600
Arc voltage (V)	60
Working gases	Ar, H_2
Working gases flow rate (L/min)	Ar:46.1, H_2:13.5%
Spray distance (mm)	120

In order to supply quantitative support for discussions of these experimental EIS results, an appropriate model (Convertor-Radiometer, France and ZSimpWin-PAR, USA) for equivalent circuit (EC) quantification has also been used. The usual guidelines for the selection of the best-fit EC were followed: a minimum number of circuit elements are employed and the χ^2 error was suitably low ($\chi^2 < 10^{-4}$), and the error associated with each element was up to 5%. Instead of pure capacitors, constant phase elements (CPE) were introduced in the fitting procedure to obtain good agreement between the simulated and experimental data (Strugaru *et al.*, 2010).

RESULTS AND DISCUSSION

Coating characterization

Fig. 1 shows the X-ray diffraction pattern of the YsZ coating and YsZ powder. In the spraying process, the temperature and the particle velocity do not involve changes in the coating crystalline structure.

The planar and cross-section SEM images of the YsZ coating are shown in Fig. 2. Note that the metallic surface is totally covered and that the coating is porous. However, the cross section SEM images demonstrate that the pore channels are not simply perpendicular to the surface. Small cracks are observed at the interface of YsZ coating on 310 austenitic stainless steel surfaces (Fig. 2B).

Electrochemical characterization

Plots in semi-logarithmic scale of current densities corresponding to YsZ-coated and uncoated NiMo samples in 3.5% NaCl solution at 25°C traced between -1000 mV to 1000 mV with 1 mV/s potential sweep rate, are displayed in Fig. 3. The average values zero corrosion potential (ZCP) and corrosion current density (i_{corr}) from polarization curves determined by the VoltaLab 4 software are presented in Table 2.

Both polarization curves are typical of a direct transition from the immunity region to the passive region. Fig. 3 clearly proves that substrate alloy had a better corrosion resistance than that of the YsZ-coated 310 austenitic stainless steel. The linear polarization curves of YsZ-coated 310 austenitic stainless steel showed a shift of ZCP to more negative value (-215 mV) compared with uncoated NiMo alloy (-688 mV). The lower ZCP exhibited for YsZ-coated 310 austenitic stainless steel probably can be associated with the porous character of this coating. For this sample the oxygen reduction chatodic reaction would be more polarized, so that the intersection of chatodic and anodic curves will take place at lower potential. It is expect that the oxygen content inside the pores is smaller than the surface. In this case the exchange current density of oxygen reduction reaction will be smaller and its cathodic reaction will become more polarized.

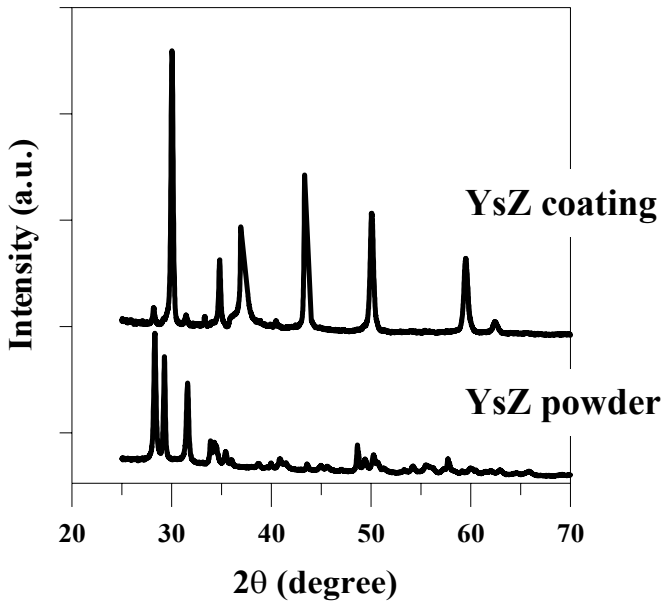

Fig. 1 – XRD patterns of YsZ powder and coating.

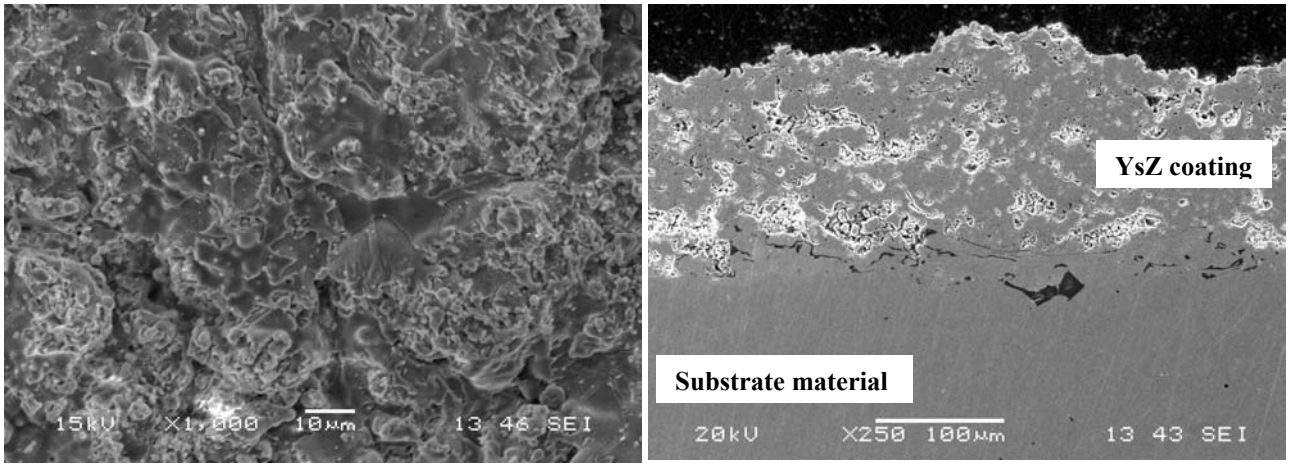

(A) (B)

Fig. 2 – Planar and cross-section SEM images of the YsZ-coated 310 austenitic stainless steel: (A) planar image, and (B) cross-section.

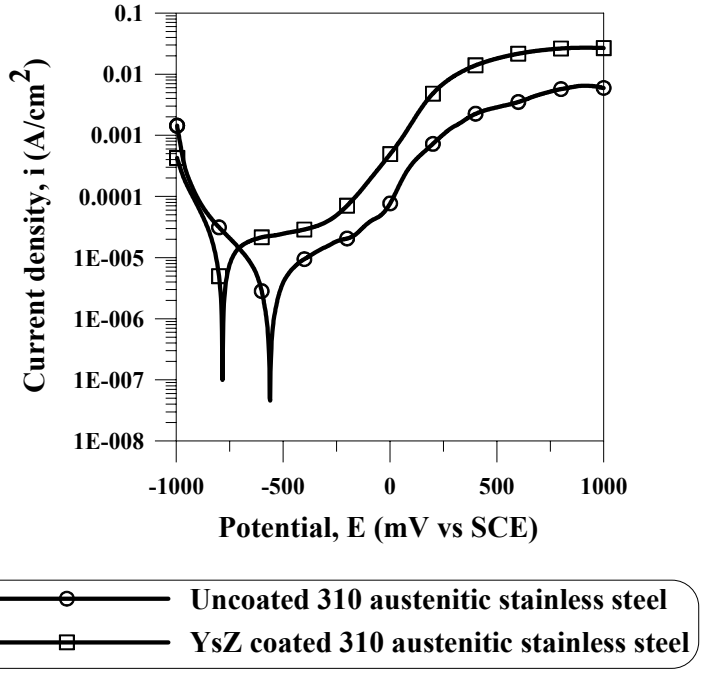

Fig. 3 – Linear potentiodynamic polarization curves measured for YsZ-coated and uncoated alloy specimens after immersion in 3.5% NaCl.

The corrosion current density was shifted to higher value (about two times higher) in case of YsZ-coated 310 austenitic stainless steel. For the uncoated 310 austenitic stainless steel, sufficient oxygen is available to maintain the surface oxide, whereas for YsZ-coated 310 austenitic stainless steel, the available oxygen present in pores is insufficient.

The susceptibility of an alloy to localized corrosion in a certain medium can be characterized in terms of the breakdown potential (Ebd) relative to the ZCP.[17,18] The potential range situated between the ZCP and Ebd represents the passivity zone in which corrosion is weak or even insignificant. Thus, the difference between the Ebd and the ZCP is commonly used as a measure of the material's susceptibility to pitting corrosion. As the difference between Ebd and ZCP becomes smaller, the alloy is expected to become more susceptible to pitting corrosion.

Table 2 lists the values of breakdown potential (Ebd) together with values calculated for Ebd-ZCP. Ebd of uncoated 310 austenitic stainless steel is around -50 mV and the passive extends up

to 500 mV. YsZ-coated 310 austenitic stainless steel Ebd of YsZ-coated 310 austenitic stainless steel is smaller around -200 mV but the passive zone is large (about 600 mV). The smaller oxygen availability inside the pores of YsZ-coated 310 austenitic stainless steel seems to favor passive film breakdown. The values of Ebd-ZCP provide a more reliable measure of the breakdown resistance. An alloy with a particular surface condition may exhibit a small Ebd but have a sufficiently negative ZCP that the difference between them is higher. Table 2 shows that YsZ-coated 310 austenitic stainless steel in 3.5% NaCl solution has a small Ebd value but its value of Ebd- ZCP is well around 600 mV.

The SEM images of coated and uncoated surface samples after linear potentiodynamic polarization test in 3.5% NaCl solution confirm the presence of localized corrosion.

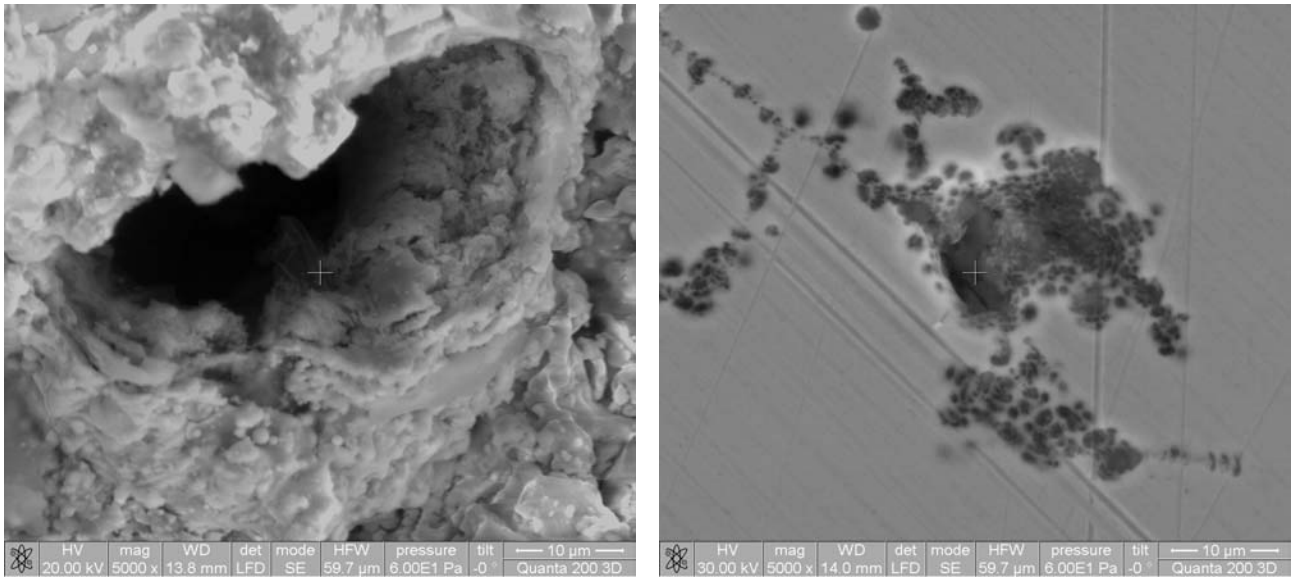

(A) (B)

Fig. 4 – SEM observation of the: (A) YsZ coated, and (B) uncoated samples after linear polarization test in 3.5% NaCl solution.

Table 2

The mean values of parameters measured and calculated for the samples in 3.5% NaCl solution (25 ^{o}C)

Sample	ZCP (mV)	i_{corr} (µA/cm2)	Ebd (mV)	Ebd -ZCP (mV)
Uncoated NiMo alloy	-784	4.1	-208	576
YsZ-coated NiMo alloy	-560	11.2	-42	518

Impedance measurements of YsZ-coated 310 austenitic stainless steel were carried out at open circuit potential conditions in 3.5% NaCl solution at 25^{o}C. The impedance spectra obtained are shown as Bode plots in Fig. 5.

According to the impedance diagram, the Bode-phase plots are in agreement with an EC with two times constant (Fig. 6a).

The impedance spectra were fitted using the Convertor and ZSimpWin software and the resultant EIS parameters are given in Table 3. The fitting quality of EIS data was estimated by both the chi-square (χ^2) test (between 10^{-4} and 10^{-5}) values and the comparison between error distribution versus frequency values (± 5% for the whole frequency range) corresponding to experimental and simulated data.

The R_1 and Q_1 parameters describe the processes occurring at electrolyte/coating layer. R_1 is the charge transfer resistance associated with the penetration of the electrolyte through the pores or micro-cracks existing in the coated layer and Q_1 correspond to capacitance of the coating layer. The low-frequency domain evidences the processes taking place at the substrate/electrolyte interface. The parameter R_2 coupled with Q_2 describes the processes at the substrate layer at the electrolyte/substrate layer interface. R_{sol} is the ohmic resistance of the electrolyte.

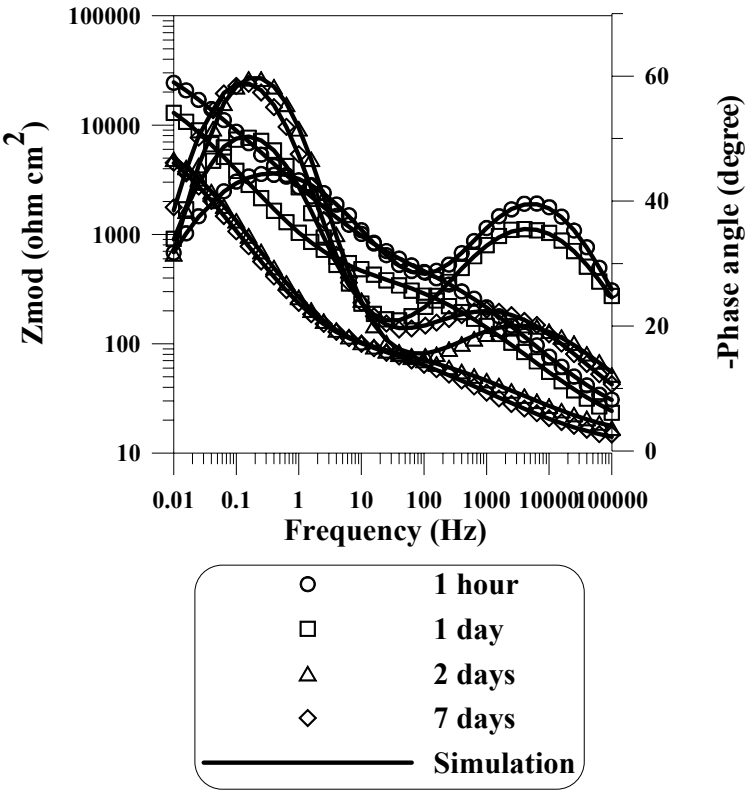

Fig. 5 – Bode plots for EIS data of YsZ-coated 310 austenitic stainless steel immersed to 3.5% NaCl solution for different exposure times.

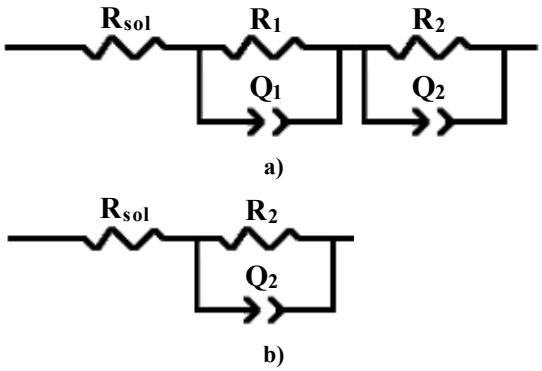

Fig. 6 – Equivalent circuits used for fitting the measured impedance spectra.

Table 3

Electrochemical parameters obtained from EIS spectra using the selected EC for the YsZ-coated 310 austenitic stainless steel after different immersion time in 3.5% NaCl solution at open circuit potential

Samples	Immersion time	10^4Q_1, S cm^{-2} s^n	n_1	$10^{-3}R_1$, Ω cm^2	10^5Q_2, S cm^{-2} s^n	n_2	$10^{-4}R_2$, Ω cm^2
YsZ-coated 310 austenitic stainless steel	1 hour	1.3	0.80	5.2	4.3	0.81	2.9
	1 day	3.5	0.80	2.9	5.6	0.81	1.4
	2 days	12.1	0.65	0.6	17.2	0.80	0.6
	7 days	53.4	059	0.5	19.4	0.80	0.6
Uncoated 310 austenitic stainless steel	1 hour	-	-	-	1.2	0.82	23.4
	1 day	2.1	0.81	6.5	4.7	0.83	9.8
	2 days	2.9	0.80	5.8	6.7	0.83	8.8
	7 days	3.4	0.80	4.2	7.3	0.82	5.9

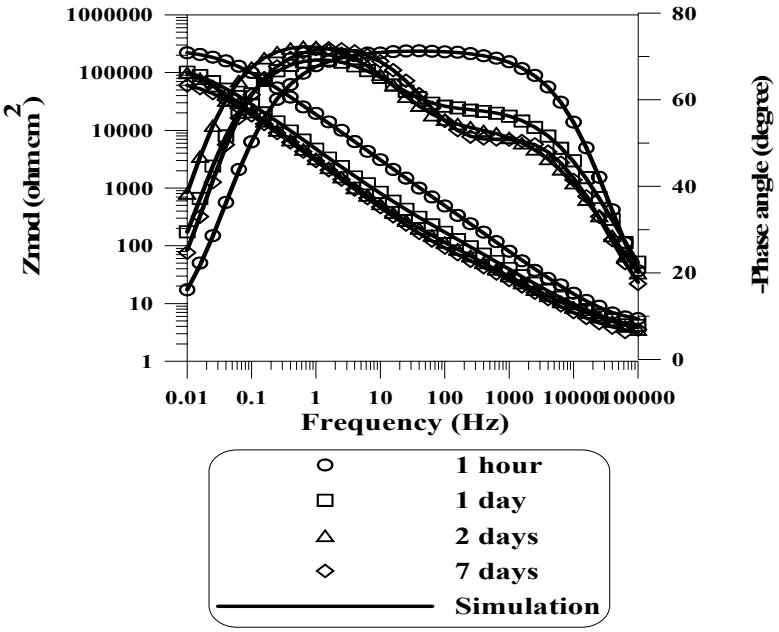

Fig. 7 – Bode plots for EIS data of 310 austenitic stainless steel immersed to 3.5% NaCl solution for different exposure times.

The decrease of R_2 as immersion time increases imply that increased number of opening pores and the coating layer became more conductive. EIS results give the experimental evidence that coatings are not very dense and present defects. However, variations of R_2 are observed during within 2 days from the time the YsZ-coated 310 austenitic stainless steel was exposed to the 3.5% NaCl solution. After that time stationary condition is achieved because no significant variations were observed for EIS parameters.

For the comparison, the EIS spectrum of the uncoated sample recorded after different immersion time in 3.5% NaCl solution at open circuit potential was also recorded and is given in Fig. 7.

According to the impedance diagram, after 1 hour immersion, only one time constant was shown. The EC (Fig. 6b) is characterized by one parallel combination terms (R_2Q_2) in series with the resistance of the solution (R_{sol}). The effect of charge transfer reaction of uncoated sample on the impedance data could be negligible. When immersion period is greater than 1 hour, the phase shift is different that 1 hour. The two peaks on uncoated sample phase angle plots indicate at least two relaxation time constants in 3.5% NaCl solution. The two relaxation time constants can be attributed to charge transfer reaction at the sample/electrolyte interface (R_1, Q_1) and to the oxide layer formed on the surface (R_2, Q_2). The values of the parameters obtained with the fitting procedure using EC presented in Fig. 6a, are reported in Table 4. Corrosion resistances are higher for uncoated material than for coated sample. Cabrini *et al.* proposed that the decrease in corrosion resistance of ceramic-coated (hydroxyapatite) substrate comparatively to uncoated may be ascribable to the presence of occluded corrosion cell formation under pores present in coated deposits. However, the polarization and EIS parameters permits to conclude that the YsZ-coated 310 austenitic stainless steel in 3.5% NaCl solution doesn't improve the electrochemical corrosion behavior of 310 austenitic stainless steel.

CONCLUSIONS

The electrochemical behavior of plasma sprayed yttrium oxide stabilized zirconium oxide (YsZ) coatings on 310 austenitic stainless steel was evaluated by means of linear polarization and EIS in 3.5% NaCl solution, at 25 ^{o}C. The YsZ coating promotes a change in electrochemical behavior of 310 austenitic stainless steel in 3.5% NaCl solution. The zero corrosion potential (ZCP) of an uncoated sample is nobler than of coated one, and the corrosion current density (i_{corr}) of coated sample is more than two times larger than that of uncoated one. Localized corrosion is likely to happen at the interface due to the porous structure of YsZ layer. EIS results give the experimental

evidence that coatings are not dense and present defects (pores and micro-cracks). Therefore, plasma sprayed coating procedures with an YsZ should be further investigated in order to minimize the existence of micro-defects in the coatings.

REFERENCES

1. K. Nishizawa, T. Miki, H. Fukaya, Y. Masuda, K. Suzuki and K. Kato, *Thin Solid Films*, **2008**, *516*, 2635-2638.
2. J.Y. Shi and H. Verweij, *Thin Solid Films*, **2008**, *516*, 3919-3923.
3. C. Piconi and G.Maccauro, *Biomaterials*, **1999**, *20*, 1-25.
4. D.E. Ruddell, B.R. Stoner and J.Y. Thompson, *Thin Solid Films*, *445*, **2003**, 14-19.
5. D. Schwingel, R. Taylor, T. Haubold, J. Wigren and C. Gualco, *Surf. Coat. Technol.*, **1998**, *108-109*, 99-106.
6. A.P. Caricato, A.D. Cristoforo, M. Fernandez, G. Leggieri, A. Luches, G. Majni, M. Martino and P. Mengucci, *Appl. Surf. Sci.*, **2003**, *208-209*, 615-619.
7. G. Carta, N.E. Habra, G. Rossetto, P. Zanella, M. Casarin, D. Barreca, C. Maragno and E. Tondello, *Surf. Coat. Technol.*, **2007**, 9289-9293.
8. Y.H Lee, C.W. Kuo, C.J. Ghih, I.M. Hung, K.Z. Fung, S.B. Wen and M.C. Wang, *Mater. Sci. Eng.* A, **2007**, *445-446*, 347-354.
9. C. Viazzi, J.P. Bonino, F. Ansart and A. Barnabe, *J. Alloys Compd.*, **2008**, *452*, 337-383
10. M.F. Morks, Y. Gao, N.F. Fahim and F.U. Yingqing, *Materials Letters*, **2006**, *60*, 1049-1053.
11. M.F. Morks, Y. Gao, N.F. Fahim, F.U. Yingqing and M.A. Shoeib, *Surface & Coating Technology*, **2005**, *199*, p. 66-71.
12. J.C. Mirza Rosca, M.V. Popa, E. Vasilescu, P. Drob, C. Vasilescu and S. I. Drob, *Rev. Roum. Chim.*, **2010**, *55*, 639.
13. V. Branzoi, M. Iordoc, F. Branzoi, G. Sbarcea and V. Marinescu, *Rev. Roum. Chim.*, **2010**, *55*, 585.
14. D. Mareci, S.I. Strugaru, C. Munteanu, R. Tarnauceanu and D. Sutiman, *Rev. Roum. Chim*., **2011**, *56*, 73.
15. F. Constantin, J.P. Millet, M. Abrudeanu and G.A. Plăiaşu, *Rev. Roum. Chim.*, **2011**, 56-917.
16. D. Mareci, G. Ciurescu, R. Chelariu, I. Cretescu and D. Sutiman, *Environmental Engineering and Management Journal*, **2010**, *9*, 81-87.
17. J.R. Scully and R.G.Kelly, "Methods for determining aqueous corrosion reaction rates", in: S.D. Cramer and B.S. Jr. Covino (Eds.) ASM Handbook, Vol 13A. Materials Park, OH: ASM International, 2003, 68.
18. G.S. Frankel, "Pitting corrosion", in: S.D. Cramer and B.S. Jr. Covino (Eds.) ASM Handbook, Vol 13A. Materials Park, OH: ASM International, 2003, 236.